Original Article

Synthesis of Rhodanine-N-acetic Acid Metal Complexes: Bioactivity of Its Iron Complex as Potential Prodrug Approach for Alzheimer's Disease

Elem Sabahsan[1], Emel Yildiz[1*], Yusuf Karatas[2]

1. Department of Chemistry, Faculty of Arts and Science, Cukurova University, Adana, Turkey.
2. Department of Medical Pharmacology, Faculty of Medicine, Cukurova University, Adana, Turkey.

*** Corresponding Author:**
Emel Yildiz, Professor.
Address: Department of Chemistry, Faculty of Arts and Science, Cukurova University, Adana, Turkey.
Phone: +90 (322) 3386084-2481
E-mail: eeyildiz@cu.edu.tr

Article info:
Received: 01 Jan 2025
Accepted: 25 Mar 2025

Keywords:
Rhodanine, Drug, Alzheimer's disease (AD), Iron, Rats

ABSTRACT

Background: Heavy metal accumulation has been shown to improve memory impairment, which is the most visible symptom of Alzheimer's disease (AD).

Objectives: This study was conducted to select and synthesize rhodanine-N-acetic acid (ROD) ligand as an azosulpha drug, as well as its metal complexes containing Fe(III), Mn(III), and Cu(II), to evaluate the iron complex's bioactivity in Swiss Albino rats.

Methods: A new series of metal complexes were synthesized and characterized using elemental analysis, magnetic susceptibility, spectroscopic, and analytical methods, including Fourier-transform infrared spectroscopy (FT-IR), inductively coupled plasma (ICP), and thermogravimetric analysis (TG). The effects of heavy metal accumulation of the characterized iron complex on rats were investigated through in vivo studies.

Results: The results indicated that as the iron load in the liver and spleen tissues increased, the iron-binding capacity of the ROD ligand also significantly increased.

Conclusion: These findings suggest that the activity of ROD metal complexes should be investigated further as a potential prodrug for AD.

Citation Sabahsan E, Yildiz E, Karatas Y. Synthesis of Rhodanine-N-acetic Acid Metal Complexes: Bioactivity of Its Iron Complex as Potential Prodrug Approach for Alzheimer's Disease. Pharmaceutical and Biomedical Research. 2025; 11(2):159-172. http://dx.doi.org/10.32598/PBR.11.2.1373

http://dx.doi.org/10.32598/PBR.11.2.1373

Introduction

Nature impacts human health from physical, chemical, biological, and socio-cultural perspectives. Paracelsus, a chemist and physician, stated that all substances present in nature are also poisons that can have a toxic effect. He pointed out that the difference between the toxicity and the therapeutic effect of a substance is related to the amount of the substance present in the human body [1-3]. From this perspective, while heavy metals sometimes cause diseases, metal complexes can also serve as treatments.

Alzheimer's disease (AD), a neurodegenerative brain disorder that causes mental and behavioral disorders, especially forgetfulness, is primarily associated with old age, and there is currently no radical solution for its treatment. However, several new treatments have shown a progress-stopping or slowing effect on the disease [4]. The harmful role of metal ions in AD has inspired research into various metal chelators, especially focusing on Zn (II), Fe(III), and Cu(II). Studies have found that increased concentrations of iron in the brains of patients with AD are significant [5].

Epidemiological studies conducted in different parts of the world have shown a relationship between aluminum levels in drinking water and AD, dementia, or cognitive damage. In post-mortem studies, it was observed that the levels of aluminum in the brain were increased in diseases, such as AD, amyotrophic lateral sclerosis, and Parkinson's disease [6-9]. Cu (II), which has a neurotoxic effect, increases Aβ accumulation in the brains of rats. In addition, increased concentrations of iron were found in the hippocampus of patients with AD in recent studies [10-13].

AD is one of the most common types of dementia in autopsy results and clinical settings. It is characterized by progressive memory loss, cognitive decline, and neuronal degeneration [14]. Epidemiological studies suggest that aluminum may not be as innocuous as previously thought and that it may actively promote the onset and progression of AD [15]. In terms of other metals, besides heavy metal accumulation, curcumin complexes of Fe (III) and Mn (II) can have positive effects on memory impairment, which is the most prominent symptom of AD. To investigate this, the effect of beta-amyloid 25-35 protein, which plays an important role in the pathology of the disease, was compared with the effects of metal complexes [16].

There are also studies investigating the drug properties of rhodamine, which demonstrate its ability to form stable complexes with Fe(III), Cu(II), Zn(II), acting as iron chelators that are useful in diseases, like AD, where metal-induced oxidative stress is a key feature [17]. While the study focuses on antibacterial activity, the enzyme inhibition and metal binding show how rhodanine scaffolds can be repurposed for multi-target strategies in neurodegeneration. Thus, it can be stated that rhodanine is a pharmacophore compatible with bioactive hybrid design, enhancing chealation and pharmacokinetic properties [18, 19]. Although there are studies of azosulpha drugs, such as anticancer, antibacterial, antiviral, and antifungal activities, very few are related to dementia as octahedral metal complexes [20, 21]. Considering all these features, it can be concluded that rhodanine is promising for the design of hybrid molecules that could potentially be applied to Alzheimer's pathology.

This study aimed to synthesize metal complexes of the Rhodanine-N-acetic acid (ROD) ligand with Fe(III), Mn(III), and Cu(II), and to evaluate the bioactivity of the iron complex in rats as an azosulpha drug. Due to restrictions on the use of experimental animals, bioactivity testing was conducted exclusively on the iron complex.

Materials and Methods

ROD, ethanol, sodium hydroxide, and physiological saline solution were purchased from Merck. Manganese(III) acetate dihydrate was purchased from Sigma-Aldrich. Iron (III) chloride was purchased from Fluka. Copper(II) chloride hexahydrate was purchased from Riedel-de-Haen. Infrared spectra were recorded using the KBr disk method with a Perkin-Elmer RX-1 Fourier-transform infrared (FT-IR) spectrometer (4000-400 cm^{-1}). Elemental analysis for carbon and hydrogen content was conducted using a Thermo Scientific Flash 2000 CHNS Analyzer. Magnetic susceptibility measurements were performed using a Sherwood Scientific device. Thermal examinations were performed on a Perkin Elmer Pyris Diamond Thermogravimetric (TG) / DTA thermal analyzer under nitrogen atmosphere at 25-800 ˚C for 10 min. Melting point determination was performed using a Gallenkamp device, and inductively coupled plasma (ICP-OES) analysis was conducted with a Perkin-Elmer Optima 2100DV ICP device.

General procedure of metal complexes

Five millimoles of iron(III) chloride, manganese acetate dihydrate and copper (II) chloride hexahydrate salts were separately dissolved in 40 mL of ethanol. Then, 10

mL of an ethanol solution containing 5.0 mmol of the ROD ligand was added in a 1:1 mole ratio. A 1 M sodium hydroxide solution was added dropwise to adjust the pH of the solutions to approximately 8-8.1, 7-7.4, and 7-7.8, respectively. The mixture was stirred at 60 ˚C for 15-20 min. Dark-brown iron (III) complex 1, dark-brown manganese complex 2 and dark purple copper (II) complex 3 precipitates were filtered off and washed several times with ethanol. The products were allowed to dry under vacuum [22].

Application of experiments on rats

Swiss Albino white male rats weighing 200-250 g, provided by the Cukurova University, Faculty of Medicine Experimental Medical Research and Application Center (CUTF-DETAUM), were used as the experimental animals in this study. The rats were placed in cages with six rats each, under standard laboratory conditions and ethical rules specified in the DETAUM directive. The application strategy for Fe-metal complex 1 is shown in Figure 1.

Experimental groups and application order

Thirty-six male Wistar albino rats, weighing between 200 and 250 g, were acquired from the Centre for Medical Research and Application (TIPDAM) at Çukurova University, Adana, Turkey. They had free access to water and chow ad libitum. All procedures were conducted according to the institutional guidelines concerning animal experimentation. The rats were divided into four different groups and treated for 10 days.

Since the number of animals that could be used was limited, only Fe metal and a single concentration could be applied. The rats were divided into four groups according to the experimental protocol. There were 6 male rats in each group. Group I (the control group) consisted of healthy rats that received an injection of 0.2 mg/kg normal saline solution (NSS). Group II was the ROD ligand group, which received an intramuscular injection of 80 mg/kg ROD. Group III received a 120 mg/kg solution of Fe(III) (Jectofer, Eczacıbaşı, Türkiye). For group IV, both 80 mg/kg ROD and 120 mg/kg Fe(III) solution were administered.

All groups were treated once a day for ten successive days. On the last day, 24 hours after the last injection, the rats were anesthetized with ether, and blood sampling was immediately done from the heart. Thereafter, the livers of the rats were removed for histopathologic examinations. The tissues were sent to pathology for examination in histopathological solution.

Histopathologic examination

The livers of the killed rats were removed and fixed in 10% neutral buffered formaldehyde solution, dehydrated in graded alcohol, and embedded in paraffin. Sections with a thickness of 3–5 μm were obtained and stained with hematoxylin-eosin (H&E). Light microscopy was used to evaluate and perform histopathologic examinations of liver sections from treated rats (H&E, 100X).

Chemicals used and application forms

In the experiments, ROD (Merck), Fe(III) solution (Jectofer, Eczacıbaşı), ROD-Fe(III) mixture, and NSS were used in effective concentrations. The application doses and forms of the chemicals are given in Table 1. A solution of 80 mg/kg ROD in NSS was administered intramuscularly to each rat at a dosage of 80 mg/kg for 10 days. The doses of the substances were determined by preliminary trials and the literature. Each experimental group consisted of six rats, and the application was conducted over 10 days. A total of 36 animals were euthanized, and during the dose adjustment, 12 of these rats died.

After all experiments, biostatistics results were examined according to iron and unsaturated iron-binding capacity (UIBC) results from blood samples taken from the four groups. SPSS software, version 20 was used for statistical analysis. Iron measurements in rats were summarized as Mean±SD. One-way analysis of variance (ANOVA) was used for the general comparison of iron measurements between groups. In cases where a significant difference was found in these analyses, Bonferroni or Tamhane tests were conducted based on whether the within-group variances were homogeneous in pairwise comparisons of the groups. Statistical significance was set at 0.05 for all tests.

Results

In this study, metal complexes of the ROD were synthesized by using Fe(III), Mn(III), Cu(II) salts and characterized by spectroscopic and analytical methods, such as ICP, FT-IR, TG, elemental analyses, and magnetic susceptibility. The theoretical and experimental results align with each other and suggest octahedral geometry for the synthesized metal complexes (Figure 2) [17, 21]. Their elemental analysis and metal percentages are listed in Table 2.

Table 1. Application doses and forms of chemicals

Chemical Name	Abbreviation	Application Dose (mg/kg)	Application Form
Normal saline solution	NSS	0.2	Intramuscular
Fe(III) solution	Fe(III)	120	Intramuscular
Rhodanine-N-acetic-acid	ROD	80	Intramuscular
Fe(III) - rhodanine-N-acetic-acid	Fe(III) –ROD	80/120	Intramuscular

PBR

Discussion

The analytical data of the complexes indicate a 1:1 mole ratio (M:L). When the magnetic susceptibility results of Fe(III), Mn(III), and Cu(II) complexes were examined, they were found to have paramagnetic properties with 5, 2, and 1 unpaired electron, respectively (Table 2).

Additionally, all of the complexes hybridized as sp^3d^2. The presence of water molecules was supported by TG analysis. The characterization of the metal complexes was also confirmed by FT-IR (section 3.1). The melting points of these complexes were above 350 ˚C. The yields (%) were 94, 85, and 40 for complexes 1, 2 and 3 respectively.

FT-IR studies

Examination of the FT-IR spectrum of ROD revealed peaks for aromatic (CH), (C=S), (CN) and (C=O) at 2984.96 cm^{-1}, 1125.13 cm^{-1}, 1311.69 cm^{-1} and 1722.35 cm^{-1}, respectively. The spectrum of complex 1 showed peaks for (OH), (CH), (C=O), (M-S), and (M-O) at 3329.72 cm^{-1}, 2971.36 cm^{-1}, 1601.50 cm^{-1}, 661.54 cm^{-1}, and 547.27 cm^{-1}, respectively. The peaks were assigned to (OH), (C=O), (M-S), and (M-O) at 3326.30 cm^{-1}, 1619.96 cm^{-1}, 720.94 cm^{-1} and 527.01 cm^{-1} for complex 2.

The peaks for compound 3 were identified as (OH), (C=O) (M-S) and (M-O) at 3664.03 cm^{-1}, 1799.76 cm^{-1}, 739.33 cm^{-1} and 524.79 cm^{-1}, respectively (Supplementary Figures S1, S2, S3 and S4).

Thermal studies

The stability of the synthesized metal complexes was determined using TG/DSC over a temperature range of 50-1000 ˚C. The TG curve of complex 1 showed a 5.8% mass loss of H_2O at 100 ˚C from outside the coordination sphere (calculated: 5.5%). The TG graph indicated a 10.1% mass loss of H_2O molecules (calculated: 9.3%). After this temperature, the thermal degradation of the organic structure began and continued up to 1000 ˚C (Figure 3).

The TG curve of complex 2 showed a mass loss from 105 ˚C to 200 ˚C in and out of the coordination sphere. After this temperature, the thermal degradation of the organic structure began and continued up to 1000 ˚C (Figure 4).

The TG curve of complex 3 showed a mass loss from 105 ˚C to 200 ˚C in and out of the coordination sphere. After this temperature, the thermal degradation of the organic structure began and continued up to 1000 ˚C (Figure 5). The analyzed results are consistent with each other.

Histological and pathological results

In vivo studies were performed in the Pharmacology Department of Medical Faculty at Cukurova University. The studies aimed to reduce the accumulation of heavy metals known to cause AD in the tissues, organs, and blood of laboratory rats.

Table 2. Elemental and ICP analysis of the synthesized complexes

Complexes	% Found				% Calculated				Molecular Weight (MW)
	C	H	N	Metal	C	H	N	Metal	(g/mol)
1	15.65	2.68	3.68	15.90	15.44	3.11	3.60	14.36	389.02
2	16.49	2.61	2.24	14.88	16.63	2.51	3.88	15.21	362.08
3	14.47	1.56	3.35	14.59	15.83	3.72	3.69	16.75	379.28

PBR

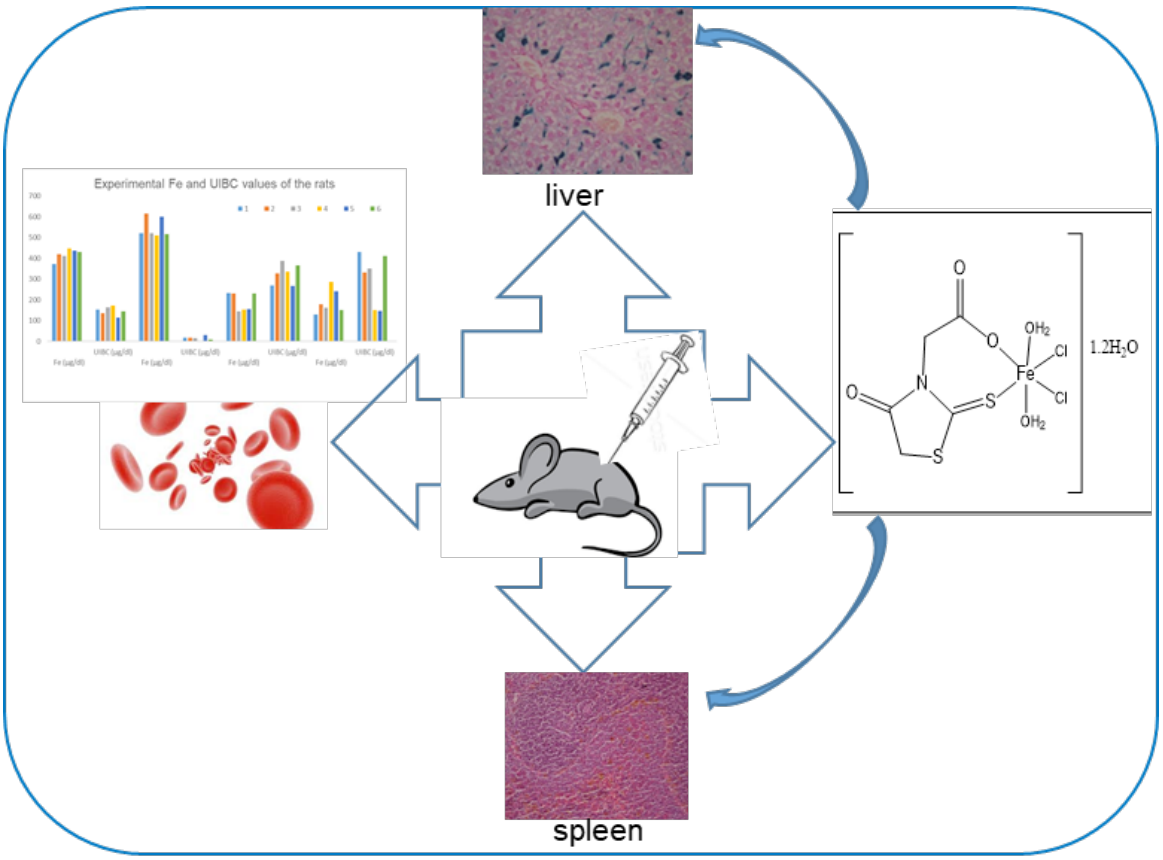

Figure 1. The application strategy for the synthesized complex shows potential prodrug properties

Pathological examination was performed to determine whether there was iron accumulation in the liver and spleen tissues of the rats (Figure 6).

In group 1 (the control group), blood congestion in the liver of the rats, as well as congestion in the spleen and enlargement of the red pulp, were observed. This indicates the presence of iron in the control group.

In group 2 (ligand loaded), patchy necrosis in the periportal area of the liver in the rats was observed, along with single-cell necrosis, degenerative changes around the central vein, significant dilatation, Kupffer cell hyperplasia, and the presence of Kupffer cells and iron pigment determined by staining with Prussian blue. In the spleen tissues, congestion, enlargement of the red pulp, and relative narrowing of the white pulp were noted. Prussian blue staining showed widespread blue pigment deposition between the lymphoid follicles. This indicates that the blue pigments are iron, and in the presence of the ligand, a significant amount of iron remains unchelated in the tissues.

Group 3 (iron loaded) exhibited excessive congestion in the liver, and excessive congestion and enlargement of the red pulp in the spleen. This indicates that the iron concentration in this group is excessive and indicates that the iron has reached the tissues.

In group 4 (iron and ligand-loaded), hemosiderosis, central vein dilation, Feat Herry degeneration, Kupffer cell hyperplasia, and ballooning degeneration were observed in the liver of the rats [23, 24]. In addition, significant cholestasis (jaundice), hemosiderin (iron), pigment deposition, and extramedullary hematopoiesis were detected. There was significant hydropic degeneration around the central vein. Prussian blue staining showed blue pigment deposition in dense sinusoids around the portal area and blue pigment deposition in yellow-brown sinusoids. Significant congestion, significant hemosiderin, enlargement of the red pulp, and relative narrowing of white pulp were observed. Congestion and accumulation of yellow-brown pigment in the spleen tissue, consisting of lymphoid follicles, were noted in the Prussian blue staining. This indicates that the blue pigments are iron, and in the presence of the ligand, the required amount of iron remains unchelated in the tissues. The accumulation of yellow-brown pigment further proves that cholestasis is also seen in spleen tissues.

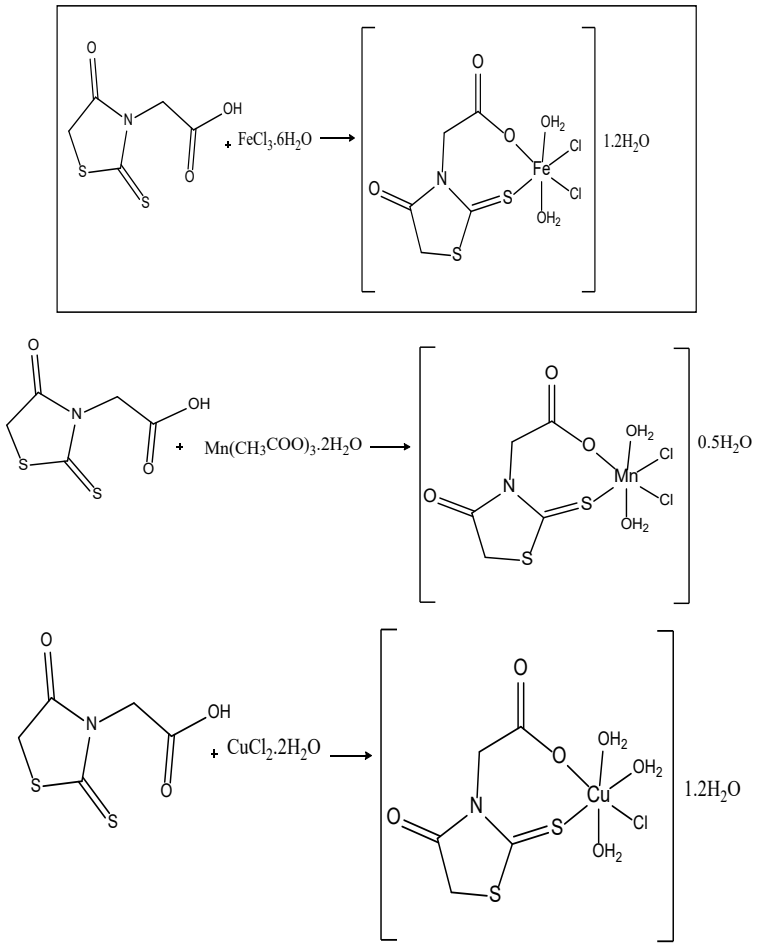

Figure 2. The proposed octahedral geometry for the synthesized complexes

PBR

As a result, observations in pathological staining among the four groups are as follows:

In group 1, iron is found only in tissues, resulting in lower iron density compared to group 3.

In group 2, iron is found in the tissues, where the ligand chelates some of this iron, while some is utilized as essential iron for tissues.

In group 3, the rat was loaded with iron in addition to the iron found in tissues; as expected, there was excessive blood congestion due to the iron reaching the tissues.

In group 4, some of the iron was chelated by the addition of ligand to the tissues with excess iron. The amount of iron in the final state is similar in groups 1 and 4. Since the ligand has a high binding capacity, it chelates the excess iron while allowing an essential amount of

The Fe (µg/dL) and UIBC (µg/dL) values in the blood of rats are shown in Table 3 and Figure 7. The values used in statistical data analysis are as follows: The amount of Fe is high in the control group and Fe-loaded groups. On the other hand, when comparing the ligand-loaded group to the ligand and Fe-loaded groups, it is supported that the binding capacity of the ligand also increases with the rise in Fe concentration, in addition to the decrease in Fe values in the blood results.

If there is a significant difference between at least two groups, ANOVA complementary calculations are carried out as shown in Table 4. According to this table, there was a difference between the four groups. In this case, a paired group comparison was made to determine the source of the difference.

One-way ANOVA post hoc data analysis was performed, as shown in Table 5, because the experimental results were significant ($P<0.001$).

According to Table 5, the control group is different from the other three groups ($P=0.001$, $P<0.001$, and $P<0.001$, respectively). The iron-loaded group is different from

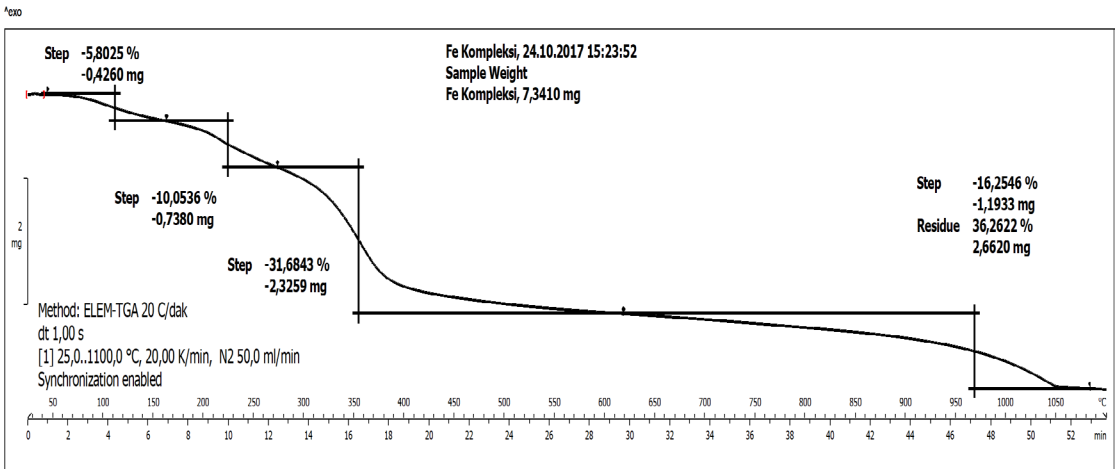

Figure 3. TG curve of complex 1

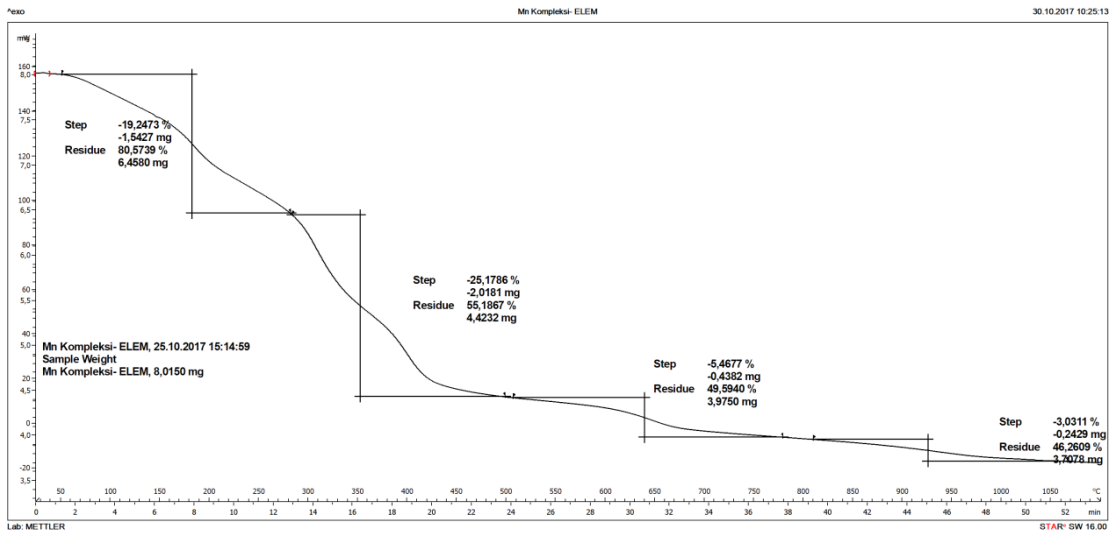

Figure 4. TG curve of complex 2

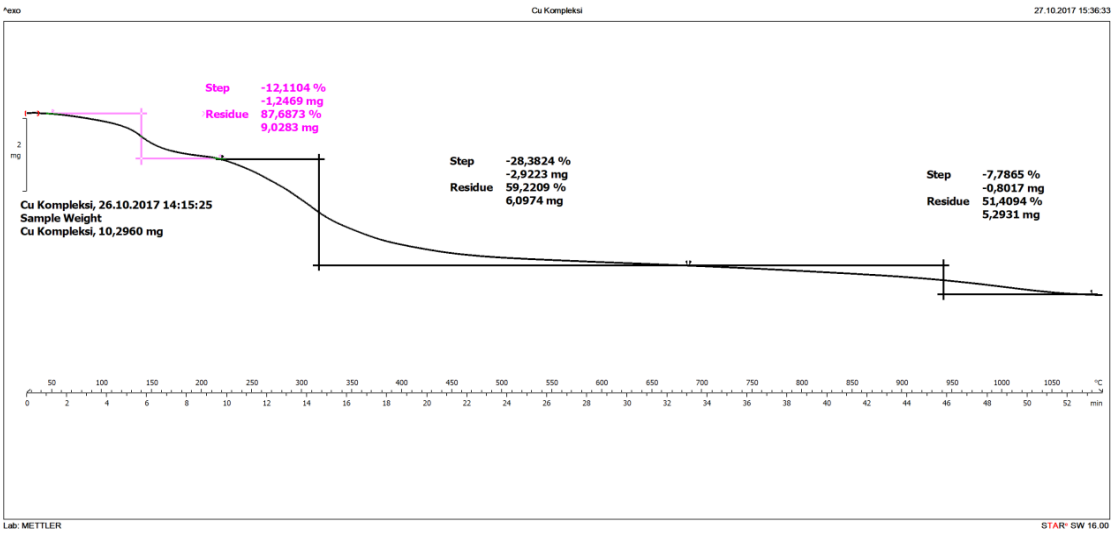

Figure 5. TG curve of complex 3

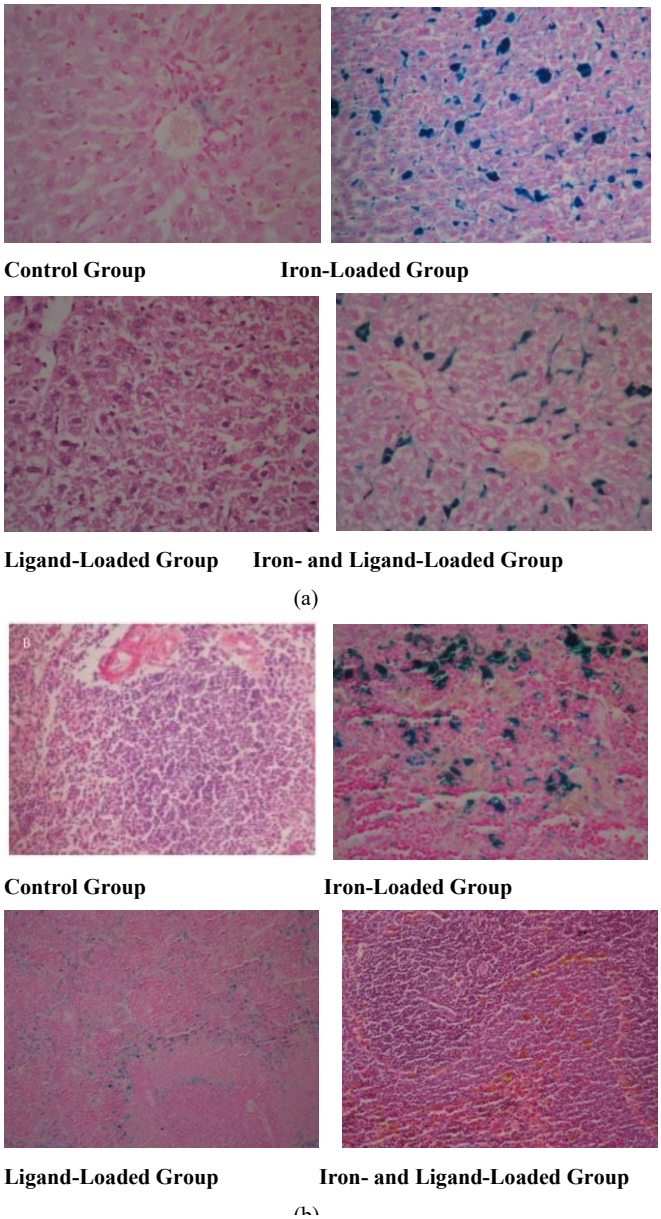

PBR

Figure 6. Pathological photographs of tissues
a) Pathological photographs of the liver, b) Pathological photographs of the spleen

ligand- and ligand- and Fe-loaded groups (P<0.001 for both). The ligand- and ligand plus Fe-loaded groups are similar (P=1.000).

Considering the biostatistics results, the control group is different from the other three groups (P=0.001, P<0.001 and P<0.001, respectively). This is only due to the iron level in peripheral blood in the control group. The iron-loaded group is different from the ligand- and ligand- and Fe-loaded groups (P<0.001 for both). This difference arises because iron is found in high concentrations and is not chelated in the iron-loaded group compared to the only ligand- and ligand- and Fe-loaded groups.

The similarity between the ligand and ligand plus Fe-loaded groups (P=1.000) was supported by hematological tests, histopathological examinations, and biostatistical results. The amount of Fe in the blood decreases when the ligand is bound. This similarity indicates that the Fe binding capacity of the ligand is higher in the presence of Fe concentration. Differences in Fe levels in peripheral blood were observed and biostatistically iden-

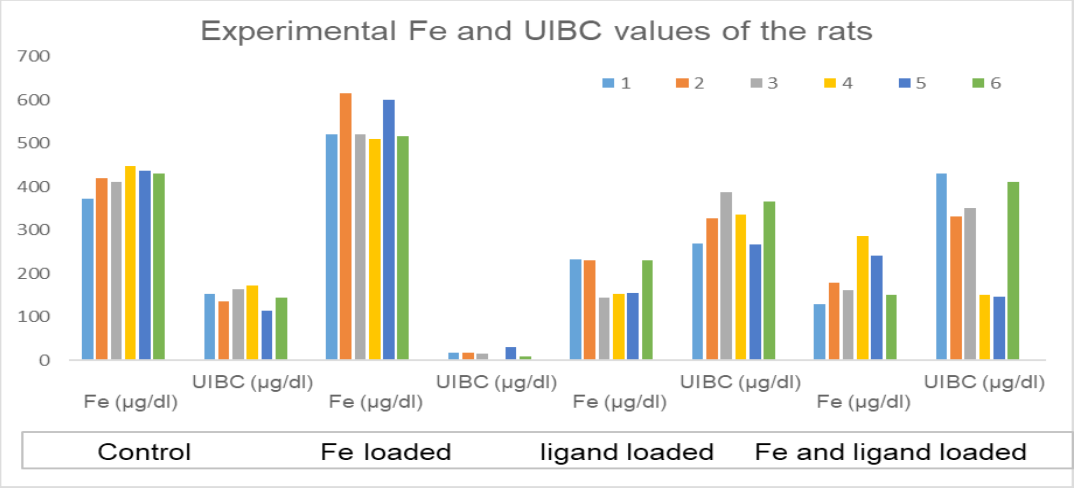

Figure 7. Graphical representation of the experimental Fe and UIBC values in rats

PBR

Table 3. Experimental Fe and UIBC values of the rats

Sample Number	Control Group		Fe-loaded Group		Ligand-loaded Group		Fe- and Ligand- loaded Group	
	Fe (µg/dL)	UIBC (µg/dL)	Fe (µg/dL)	UIBC (µg/dL)	Fe (µg/dL)	UIBC (µg/dL)	Fe (µg/dL)	UIBC (µg/dL)
1	372	153	520	18	233	270	130	430
2	420	136	615	18	231	327	180	332
3	412	164	521	16	144	387	162	352
4	447	172	510	2	154	337	287	151
5	437	115	600	30	156	268	242	147
6	430	145	517	10	230	367	151	411

UIBC: Unsaturated iron-binding capacity.

PBR

tified between the ligand-loaded group without Fe and the ligand plus Fe-loaded group. This result suggests that the Fe binding capacity may increase when the Fe load of the ligand increases.

According to the multiple comparisons tests loaded ligand and ligand and Fe, results were found to be biostatistically similar in terms of Fe binding capacity between the control group and ligand and Fe group (P=0.081). Although there is an overload of Fe in the ligand- and Fe-loaded group, only Fe is present in the body in the control

Table 4. Experimental one-way ANOVA biostatistics results

Groups	No.	Value	Std. Deviation	Std. Error	95% Reliability Between Values		Min	Max
					Lower Limit	Upper Limit		
Control	6	419.67	26.402	10.779	391.96	447.37	372	447
Iron-loaded	6	547.17	47.131	19.241	497.71	596.63	510	615
Ligand-loaded	6	191.33	44.017	17.97	145.14	237.53	144	233
Ligand- and Fe- loaded	6	192	60.156	24.559	128.87	255.13	130	287
Total	24	337.54	161.764	33.02	269.23	405.85	130	615

PBR

Table 5. Biostatistical data results of post hoc multiple comparisons

(I) Groups	(J) Groups	Mean Difference (I-J)	Std. Error	Sig.	95% Reliability Interval	
					Lower Limit	Upper Limit
Control	Iron-loaded	-127.5*	26.575	0.001	-205.29	-49.71
	Ligand-loaded	228.333*	26.575	0.000	150.55	306.12
	Ligand- and Fe- loaded	227.667*	26.575	0.000	149.88	305.45
Iron loaded	Control	127.5*	26.575	0.001	49.71	205.29
	Ligand-loaded	355.833*	26.575	0.000	278.05	433.62
	Ligand- and Fe- loaded	355.167*	26.575	0.000	277.38	432.95
Ligand-loaded	Control	-228.333*	26.575	0.000	-306.12	-150.55
	Iron-loaded	-355.833*	26.575	0.000	-433.62	-278.05
	Ligand- and Fe- loaded	-0.667	26.575	1.000	-78.45	77.12
Ligand- and Fe-loaded	Control	-227.667*	26.575	0.000	-305.45	-149.88
	Iron-loaded	-355.167*	26.575	0.000	-432.95	-277.38
	Ligand-loaded	0.667	26.575	1.000	-77.12	78.45

*The mean difference is significant at the 0.05 level.

PBR

group. The final Fe levels are similar in the control group and the overloaded Fe group due to the high metal-binding activity of the ligand. This suggests that, since the binding capacity of the ligand is high in the overloaded Fe group, the amount of Fe is comparable in both the overloaded Fe and control groups in the final analysis.

Conclusion

In this study, Fe(III), Mn(III) and Cu(II) complexes of ROD ligand were synthesized in octahedral geometry. The theoretical and experimental results for the characterization were found to be compatible with each other. Considering the analysis findings and literature information, the most suitable geometry for the compounds was proposed. After the pharmacological examination of the synthesized metal complex in terms of iron, it was observed and detected biostatistically that the iron binding capacity of the ligand is higher in cases where iron density increases, particularly in terms of iron levels in the peripheral blood between groups 2 and 4. This result indicates that the iron binding capacity of the ligand may increase when the iron load increases.

This study will contribute to the elucidation of interactions in living systems and the production of synthetic drugs if the new azosulfa drug derivatives to be synthesized exhibit biochemical and pharmacological activities. By demonstrating the ligand's potential in modulating iron binding, the study opens avenues for future research into novel drug derivatives that could offer therapeutic benefits in managing iron-related disorders.

Ethical Considerations

Compliance with ethical guidelines

The study was approved by the Ethics Committee of Cukurova University, Adana, Turkey (Code: Ç.Ü.T.F.-DETAUM-5).

Funding

This study was financially support by the Research Unit of Çukurova University, Adana, Turkey (Grant No.: FYL-2015-2531).

Authors' contributions

Supervision: Emel Yildiz; Data collection, investigation, and writing: All authors; Data analysis: Elem Sabahsan and Emel Yildiz.

Conflict of interest

The authors declared no conflict of interest.

Acknowledgments

The authors gratefully acknowledge financial support from the Research Unit of Çukurova University, Adana, Turkey.

References

[1] Güven A, Kahvecioğlu Ö, Kartal G, Timur S, Metalurji İT. Metallerin çevresel etkileri-III. Metalurji Dergisi. 2004; 138:64-71. [Link]

[2] Tchounwou PB, Yedjou CG, Patlolla AK, Sutton DJ. Heavy metal toxicity and the environment. Exp Suppl. 2012; 101:133-64. [DOI:10.1007/978-3-7643-8340-4_6] [PMID]

[3] Pokras M. Essentials of medical geology: Impacts of the natural environment on public health. Environ Health Perspect. 2005; 113(11):A780. [DOI:10.1289/ehp.113-a780a]

[4] Nelson L, Tabet N. Slowing the progression of Alzheimer's disease: What works? Ageing Res Rev. 2015; 23(Pt B):193-209. [DOI:10.1016/j.arr.2015.07.002] [PMID]

[5] Telpoukhovskaia MA, Rodríguez-Rodríguez C, Scott LE, Page BD, Patrick BO, Orvig C. Synthesis, characterization, and cytotoxicity studies of Cu(II), Zn(II), and Fe(III) complexes of N-derivatized 3-hydroxy-4-pyridiones. J Inorg Biochem. 2014; 132:59-66. [DOI:10.1016/j.jinorgbio.2013.12.003] [PMID]

[6] Müller D, Desel H. Common causes of poisoning: Etiology, diagnosis and treatment. Dtsch Arztebl Int. 2013; 110(41):690-9. [DOI:10.3238/arztebl.2013.0690]

[7] Garofalo M, Pandini C, Bordoni M, Pansarasa O, Rey F, Costa A, et al. Alzheimer's, parkinson's disease and amyotrophic lateral sclerosis gene expression patterns divergence reveals different grade of RNA Metabolism Involvement. Int J Mol Sci. 2020; 21(24):9500. [DOI:10.3390/ijms21249500] [PMID]

[8] Roemhild K, von Maltzahn F, Weiskirchen R, Knüchel R, von Stillfried S, Lammers T. Iron metabolism: Pathophysiology and pharmacology. Trends Pharmacol Sci. 2021; 42(8):640-56. [DOI:10.1016/j.tips.2021.05.001] [PMID]

[9] Düzel E, Costagli M, Donatelli G, Speck O, Cosottini M. Studying alzheimer disease, parkinson disease, and amyotrophic lateral sclerosis with 7-T magnetic resonance. Eur Radiol Exp. 2021; 5(1):36. [DOI:10.1186/s41747-021-00221-5] [PMID]

[10] Rivera-Mancía S, Pérez-Neri I, Ríos C, Tristán-López L, Rivera-Espinosa L, Montes S. The transition metals copper and iron in neurodegenerative diseases. Chem Biol Interact. 2010; 186(2):184-99. [DOI:10.1016/j.cbi.2010.04.010] [PMID]

[11] Ferrada E, Arancibia V, Loeb B, Norambuena E, Olea-Azar C, Huidobro-Toro JP. Stoichiometry and conditional stability constants of Cu(II) or Zn(II) clioquinol complexes: implications for Alzheimer's and Huntington's disease therapy. Neurotoxicology. 2007; 28(3):445-9. [DOI:10.1016/j.neuro.2007.02.004] [PMID]

[12] Ihalainen J, Sarajärvi T, Rasmusson D, Kemppainen S, Keski-Rahkonen P, Lehtonen M, et al. Effects of memantine and donepezil on cortical and hippocampal acetylcholine levels and object recognition memory in rats. Neuropharmacology. 2011; 61(5-6):891-9.[DOI:10.1016/j.neuropharm.2011.06.008] [PMID]

[13] Cruz-Alonso M, Fernandez B, Navarro A, Junceda S, Astudillo A, Pereiro R. Laser ablation ICP-MS for simultaneous quantitative imaging of iron and ferroportin in hippocampus of human brain tissues with Alzheimer's disease. Talanta. 2019; 197:413-21. [DOI:10.1016/j.talanta.2019.01.056] [PMID]

[14] Zhu F, Qian C. Berberine chloride can ameliorate the spatial memory impairment and increase the expression of interleukin-1beta and inducible nitric oxide synthase in the rat model of Alzheimer's disease. BMC Neurosci. 2006; 7:78. [DOI:10.1186/1471-2202-7-78] [PMID]

[15] Bondy SC. Prolonged exposure to low levels of aluminum leads to changes associated with brain aging and neurodegeneration. Toxicology. 2014; 315:1-7. [DOI:10.1016/j.tox.2013.10.008] [PMID]

[16] Bicer N, Yildiz E, Yegani AA, Aksu F. Synthesis of curcumin complexes with iron(III) and manganese(II), and effects of curcumin-iron(III) on Alzheimer's disease. New J Chem. 2019; 42(10):8098-104. [DOI:10.1039/C7NJ04223J]

[17] El-Sonbatı AZ, Diab MA, El-Bindary AA, Morgan SHM. Coordination chemistry of supramolecular rhodanine azodye sulphadrugs. Inorganica Chim Acta. 2013; 404:175-87. [DOI:10.1016/j.ica.2013.04.001]

[18] Zinglé C, Tritsch D, Grosdemange-Billiard C, Rohmer M. Catechol-rhodanine derivatives: specific and promiscuous inhibitors of Escherichia coli deoxyxylulose phosphate reductoisomerase (DXR). Bioorg Med Chem. 2014; 22(14):3713-9. [DOI:10.1016/j.bmc.2014.05.004] [PMID]

[19] Li C, Liu JC, Li YR, Gou C, Zhang ML, Liu HY, et al. Synthesis and antimicrobial evaluation of 5-aryl-1,2,4-triazole-3-thione derivatives containing a rhodanine moiety. Bioorg Med Chem Lett. 2015; 25(15):3052-6. [DOI:10.1016/j.bmcl.2015.04.081] [PMID]

[20] Refat MS. Synthesis and characterization of ligational behavior of curcumin drug towards some transition metal ions: Chelation effect on their thermal stability and biological activity. Spectrochim Acta A Mol Biomol Spectrosc. 2013; 105:326-37. [DOI:10.1016/j.saa.2012.12.041] [PMID]

[21] El-Bindary AA, El-Sonbati AZ, Ahmed RM. Coordination modes of novel rhodanine azodye complexes. Spectrochim Acta A Mol Biomol Spectrosc. 2002; 58(2):333-9. [DOI:10.1016/S1386-1425(01)00538-8] [PMID]

[22] Guzzo MB, Nguyen HT, Pham TH, Wyszczelska-Rokiel M, Jakubowski H, Wolff KA, et al. Methylfolate trap promotes bacterial thymineless death by sulfa drugs. Plos Pathog. 2016; 12(10):e1005949. [DOI:10.1371/journal.ppat.1005949] [PMID]

[23] Itoshima T, Kiyotoshi S, Kawaguchi K, Ogawa H, Ohta W, Ito T, et al. Kupffer cell hyperplasia in liver diseases. Demonstration by scanning electron microscopy of biopsy samples. Gastroenterol Jpn. 1981; 16(3):223-31. [DOI:10.1007/BF02815801] [PMID]

[24] Hoeft K, Bloch DB, Graw JA, Malhotra R, Ichinose F, Bagchi A. Iron loading exaggerates the inflammatory response to the toll-like receptor 4 ligand lipopolysaccharide by altering mitochondrial homeostasis. Anesthesiology. 2017; 127(1):121-35. [DOI:10.1097/ALN.0000000000001653] [PMID]

Supplementary: FT-IR spectra for ligand and the synthesized complexes

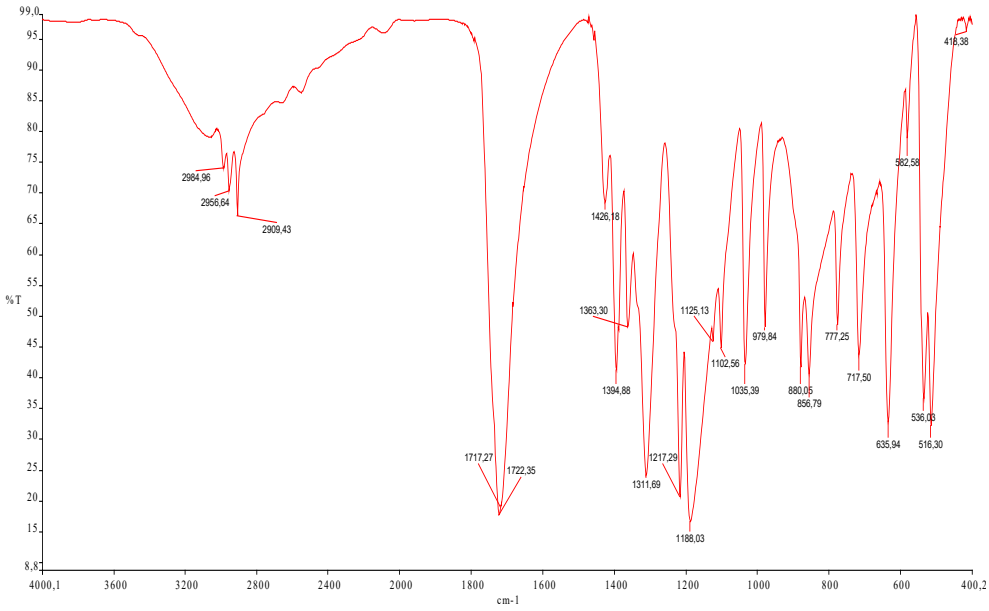

Figure S1. FT-IR spectrum for rhodanin-N-acetic acid

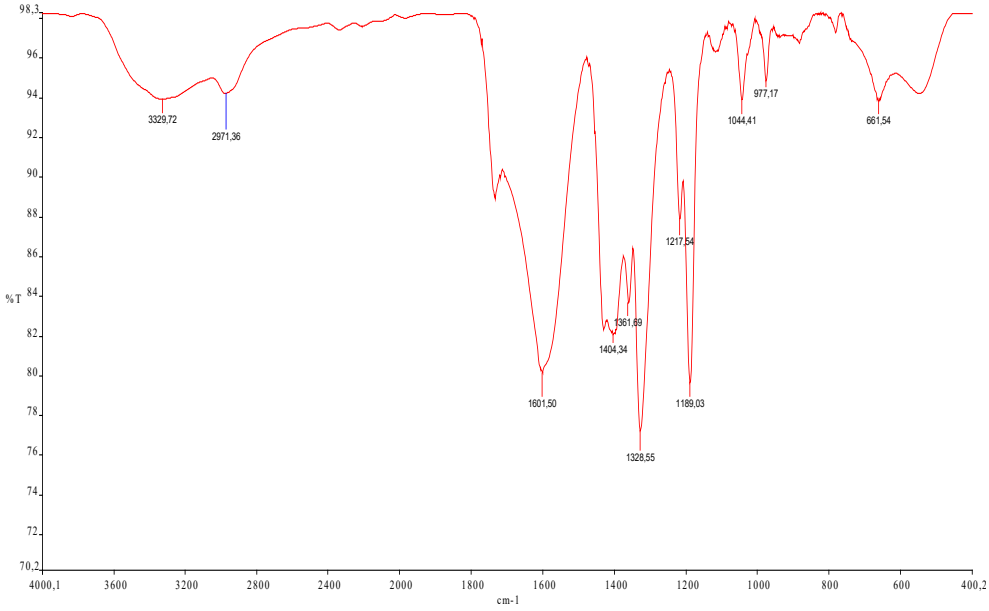

Figure S2. FT-IR spectrum for 1

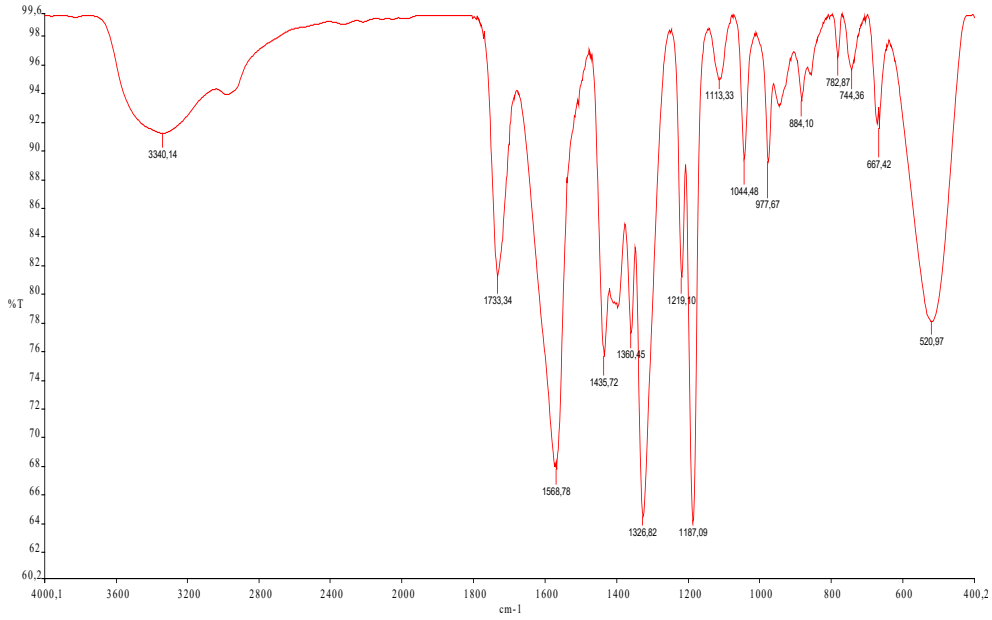

Figure S3. FT-IR spectrum for 2

PBR

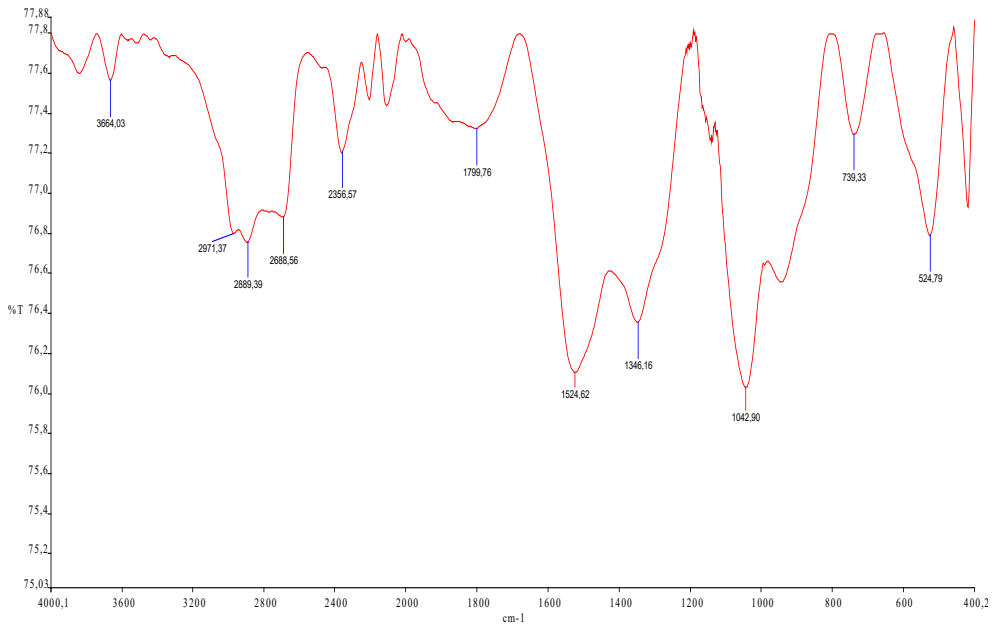

Figure S4. FT-IR spectrum for 3

PBR